Relating hippocampal subfield microstructure to delayed verbal memory in cognitively intact individuals at genetic risk for developing Alzheimer's disease

Jennapher Lingo VanGilder*, Ph.D.[1]; Andrew Hooyman*, Ph.D.[2]; Sasha Hakhu*, Ph.D.[1]; Kurt G. Schilling, Ph.D.[3]; Leland S. Hu, M.D.[4]; Yuxiang Zhou, Ph.D.[5]; Richard J. Caselli, M.D.[6]; Leslie C. Baxter, Ph.D.[7]; Scott C. Beeman, Ph.D.[1]

[1]School of Biological and Health Systems Engineering, Arizona State University; [2]Department of Physical Therapy, Chapman University, Irvine, CA; [3]Vanderbilt University Institute of Imaging Science, Vanderbilt University, Nashville, TN; [4]Department of Radiology, Mayo Clinic, Phoenix, AZ; [5]Department of Medical Physics, Mayo Clinic, Phoenix, AZ; [6]Department of Neurology, Mayo Clinic, Phoenix, AZ; [7]Department of Psychiatry & Psychology, Mayo Clinic, Phoenix, AZ

*These authors have contributed equally to this paper.

Corresponding Author: Scott C. Beeman, Ph.D.

scott.beeman@asu.edu

(480) 727-9061

Abstract

Early intervention to delay Alzheimer's disease (AD) is critical but detecting at-risk individuals before disease progression is challenging. We evaluate the relationship between hippocampal microstructure and memory in cognitively intact older adults based on the at-risk APOE ε4 genotype. Participants (n=41 noncarriers, 33 carriers) ≥ 60 years (mean±SD: carriers 71±6.6; noncarriers 71±6.4) were compared using the diffusion weighted MRI microstructure measures (Neurite Orientation Dispersion and Density Imaging; NODDI), diffusion tensor imaging (DTI), volumetric measures and memory scores. Regression analyses indicated that while volumetric data showed no significant findings, the orientation dispersion (ODI) in the left subiculum was positively associated with verbal memory only in APOE ε4 carriers (FDR-corrected p=0.01) but not in noncarriers or for other volumetry or for visual memory. The right hemisphere did not show significant memory correlations. Hippocampal microstructure, rather than volume, may provide early insights into early memory changes in groups at risk for AD.

Introduction

New treatments to delay Alzheimer's Disease (AD) symptoms are highlighting the need for sensitive noninvasive measures to detect and track brain function (Nelson and Tabet, 2015). A major challenge of this treatment strategy has been the inability to accurately detect at-risk individuals prior to significant disease progression. The apolipoprotein epsilon 4 (APOE ε4) allele is a common genetic AD risk factor, associated with synaptic toxicity and eventual neuronal loss (Hesse et al., 2019; Lane-Donovan and Herz, 2017) through beta amyloid protein accumulation (Koffie et al., 2012; Sheng et al., 2012). AD pathogenesis hypotheses posit that the hippocampus becomes functionally disconnected from neural networks due to synaptic loss (Kashyap et al., 2019; Li and Selkoe, 2020), pathology begins within left hemispheric structures (e.g., the hippocampal complex (Abraham et al., 2020; Jessen et al., 2006; Mohtasib et al., 2022)), and delayed verbal memory is one of the first cognitive functions to demonstrate impairment in APOE ε4 carriers (Caselli et al., 2009). Reduced functional connectivity of the left (but not right) hippocampus was significantly related to decline in delayed verbal memory performance in cognitively intact APOE ε4 carriers, independent of hippocampal volumes, nonverbal memory change, and was not observed in noncarriers (Baxter et al., 2023). These findings suggest that pathological changes in left hippocampal functional connectivity occur earlier than hippocampal volume and prior to frank behavioral impairment in at-risk individuals. Since APOE ε4 carriers may experience exacerbated synapse loss it is plausible that the functional hippocampal disconnection may be due to a loss of synaptic connections although the microstructural correlates of this brain-behavioral relationship have not been well-described in the cognitively intact.

Considering the hippocampus as a singular neural region may be insensitive for detection of disease-specific effects given that subregions (or subfields) within the hippocampus are histologically (Adler et al., 2014; Flores et al., 2020) and functionally (Chang et al., 2021; Zammit et al., 2017) distinct, and that hippocampal subfields (i.e., the cornu ammonis (CA) 1, CA2-3, CA4-dentate gyrus, and the subiculum) may be differentially impacted by AD-related pathology. Volumetric studies have linked subicular atrophy to declines in delayed verbal memory (Lindberg et al., 2017) and conversion from mild cognitive impairment to AD (Abraham et al., 2020; Carlesimo et al., 2015; Hett et al., 2019; Zhao et al., 2019), whereas others suggest that

CA1 atrophy may be the best indicator of conversion to AD (Apostolova et al., 2006; de Flores et al., 2015). Combining areas may mask emerging hippocampal subfield changes in at risk individuals. Whether subfield *microstructure* in APOE ε4 carriers is related to memory performance is less studied and may confer greater sensitivity to subtle early changes.

Quantitative multi-shell diffusion magnetic resonance imaging (dMRI) can be made exquisitely sensitive to the underlying microstructure of dendrites and axons (i.e., components of the synapse) through rational sampling of the dMRI parameter space and biophysical modeling of diffusion properties within brain tissues. DTI and Neurite Orientation Dispersion and Density Imaging (NODDI) are two methods to assess white matter anatomy. While DTI is the clinical standard-of-care model used to calculate diffusion metrics of fractional anisotropy (FA, a measure of white matter integrity), and radial diffusivity (RD, a measure of diffusion especially in the radial direction of a white matter tract), it lacks specificity because various microstructural alterations such as demyelination or axonal loss can impact the RD metric (Jelescu et al., 2020) rendering the underlying physiological mechanism unclear. Advanced diffusion models like NODDI offer metrics like neurite density index (NDI) and orientation dispersion index (ODI) (Qiu et al., 2017) where NDI is a direct measure of the density of neurites (axons and dendrites) and ODI quantifies the degree of dispersion of axon orientations. These measures can help capture changes in tissue microstructure that may not be detected by traditional models, particularly in areas with complex fiber architecture. ODI correlates with PET-based measures of synaptic density (Kohli et al., 2021; Mak et al., 2021) and both NODDI metrics have been shown to distinguish individuals with mild cognitive impairment from those with AD (Fu et al., 2020; Vogt et al., 2020), but whether it can be used to identify microstructural degeneration in asymptomatic at-risk groups is unknown.

We systematically evaluated if structural measures of specific hippocampal subfields were associated with memory in cognitively intact groups with differing AD risk. Based on prior work showing earlier left hemisphere changes (Thompson et al., 2003), we hypothesized that reduced left hippocampal microstructure would be associated with reduced delayed verbal memory scores in APOE ε4 carriers. Given that volumetric studies suggest the subiculum is first to show structural changes (Chi et al., 2022; Zammit et al., 2017), we

hypothesized that NODDI-based measures the left subiculum microstructure would preferentially predict memory performance in cognitively intact APOE ε4 carriers.

Methods

Experimental procedures were approved by the Institution's Review Board and adhered to the Declaration of Helsinki. Participants provided informed consent prior study enrollment. Data were collected as part of the longitudinal AZ APOE study by the Mayo Clinic in Arizona (see Caselli et al., 2011, 2010)). Neuroimaging and cognitive data from 74 community-dwelling adults (carriers n=41; noncarriers n=33) with mean ± SD age of 71±6.6 and 71±6.4 years, respectively, were retrospectively. Cognitively intact status was determined by MMSE (Folstein et al., 1975), Instrumental Activities of Daily Living Questionnaire (Katz et al., 1970), and Hamilton Depression Rating Scale (Hamilton, 1967). A licensed neuroradiologist, neurologist, and neuropsychologist screened for presence of confounding medical, neurological, and/or psychiatric disorders and conversion to mild cognitive impairment. To minimize any age-related structural effects, we included participants ≥ 60 year. Verbal memory score was the delayed recall measure from the Rey Auditory Verbal Learning Test (AVLT-DR) due to its sensitivity to early changes in preclinical AD (Caselli et al., 2009). Since verbal-visual memory show left-right hemisphere predominance, respectively, we also examined delayed recall visual memory scores from the Rey-Osterrieth Complex figure test (CFT-DR;). Cognitive and imaging data were collected within a few weeks of each other.

MRI acquisition and preprocessing

A Siemens 3T MRI Skyra scanner was used to obtain multi-shell diffusion-weighted images via an EPI sequence with parameters: b-values = 0.5, 1, and 2 ms/μm^2 with 6, 38, and 47 diffusion encoding directions, respectively, and nine interleaved b=0 volumes; TR/TE: 4.3/0.101 s; flip-angle = 90°; 2x2x2 mm^3 spatial resolution; slice thickness: 2.0 mm; scan time 7.87 minutes. T1-weighted images with parameters: TR/TE: 6.7/3.1 s, flip-angle=9°, FOV=256 mm, 1x1x1 mm^3 spatial resolution, 208 sagittal slices were used to nonlinearly align images during the coregistration process and for volumetry. FSL (FMRIB, Oxford, UK) was used to reduce noise (dwidenoise), susceptibility-induced distortion (Schilling et al., 2020), to create a whole

brain mask to extract brain from non-brain tissues (dwi2mask) and to correct for motion and eddy currents (eddy). To account for the rotational component of registration, the b-vector files were compensated after motion correction and prior to calculating the b matrices. B1-field inhomogeneity across all diffusion volumes was then corrected for (dwibiascorrect) in MRtrix (Tournier et al., 2019).

Neurite Orientation Dispersion and Density Imaging (NODDI) modeled dMRI to quantify net density (neurite density index, NDI) and orientation (orientation dispersion index, ODI) of dendrites and axons within each voxel (Zhang et al., 2012) using MATLAB (MathWorks, Inc.). ODI generates values from 0 to 1 and is interpreted as a measure of neurite coherence with values closer to 1 suggesting that the net orientation of neurites within that voxel is widely dispersed and values closer to 0 suggests that net orientation has coherence in a uniform direction. NDI is the volume fraction of tissue that comprises neurites, or neurite density, where values closer to 1 would suggest that the intravoxel tissue is comprised largely of neurites. We also calculated fractional anisotropy (FA) and mean diffusivity (MD) maps using the standard of care DTI model (FSL's DTIFIT tool).

Each participant's b0 image was nonlinearly transformed to their structural T1-weighted image (FSL's fnirt), which was then nonlinearly transformed to the Montreal Neurological Institute 152 (MNI) standard brain atlas. Bilateral hippocampi (Harvard-Oxford cortical and subcortical structural atlases (Desikan et al., 2006; Frazier et al., 2005; Makris et al., 2006)) and subfields (i.e., the cornu ammonis (CA) 1, CA 2-3, CA 4-dentate gyrus, and the subiculum (Iglesias et al., 2015)) were included as hippocampal regions of interest (ROIs). To account for age-related differences in brain structure such as ventricular expansion (Gordon et al., 2013), ROIs were nonlinearly transformed to an older adult brain atlas (described in (Gordon et al., 2015)) and then to participant native diffusion space. To constrain to only gray matter voxels, ROIs were thresholded by each participant's grey matter tissue mask (FAST). Volume (fslstats) and NODDI indices were quantified for each ROI and the tissue-weighted mean was calculated to reduce estimation bias caused by partial volume effects (Parker et al., 2021)., A tissue-weighted mean approach (Parker et al., 2021) addressed cerebrospinal fluid (CSF) contamination in our ROI analysis. Traditional methods calculate the mean NODDI metric by averaging all voxels in an ROI, which can be biased by CSF contamination. Our method uses tissue fraction metrics from

NODDI to account for varying CSF contamination across voxels, providing a more accurate representation of regional microstructure. This approach corrects for CSF partial volume effects while maintaining the intent of estimating the average microstructure within the tissue of the ROI.

Statistical analysis

Statistical analyses were performed in R Version 2024.04.2+764 (2024.04.2+764) with iterative linear regression models to evaluate the extent to which APOE ε4 status predicts the relationship between hippocampal regions and memory. Participant allelic group (APOE ε4 carrier/noncarrier), diffusion imaging metrics (for example, ODI or FA) for each region of interest (ROI), and their interaction as predictor variables for AVLT-DR and CFT-DR scores were entered with age as a covariate to account for age-related differences in tissue microstructure. Separate regressions were performed for imaging metrics across each ROI corrected for multiple comparisons using false discovery rate (FDR). For any significant hippocampal region-by-APOE ε4 status interaction, a follow-up sensitivity analysis was conducted to assess whether the same relationship persisted when considering the volumetric measure of the hippocampal region to determine whether the microstructural metrics (ODI or NDI) were better at detecting the influence of APOE ε4 status on cognitive performance compared to volume. Additionally, p-values from the APOE interaction were log-transformed and plotted across the 10 hippocampal ROIs for FA, ODI, and volume metrics in relation to CFT recall and AVLT scores, with Bonferroni threshold for 10 tests (alpha = .005) applied to assess significance.

Results

In our analysis of the APOE interaction across 10 hippocampal regions of interest, including left and right CA1, CA2-3, CA4, subiculum, and the whole hippocampus, we assessed FA, ODI, and volumetric metrics in relation to AVLT-DR and CFT-DR scores. Demographic and NODDI data are summarized in Table 1.

The log-transformed p-values revealed that the left subiculum showed a statistically significant interaction with AVLT scores after Bonferroni correction ($p<0.005$) (Figure 1). Further comparison between APOE ε4 carriers and noncarriers showed lower left subiculum ODI (z-score) correlated with lower verbal memory scores in carriers but not in noncarriers (Figure 2). No associations between right hippocampus and memory performance, hippocampal volume for either side were observed. Statistical results of these

relationships between imaging metrics and cognitive scores based on carrier status are summarized in Tables 2 and 3. Supplementary analyses demonstrated a significant but weaker relationship between DTI-FA and memory compared to NODDI-Kappa (a component measure of neurite orientation dispersion) within the left subiculum, highlighting the greater sensitivity of NODDI in detecting early hippocampal microstructural changes (Figure S1).

Discussion

This study found that decreased hippocampal microstructure as measured by the NODDI ODI metric was associated with worse verbal memory performance only in older cognitively intact adults carrying the APOE ε4 allele but not in noncarriers. This association was for the left but not right hippocampus and there was no association of microstructural measures with visual memory. FA showed the same general trend, but was less robust (and nonsignificant) compared to ODI. Furthermore, these associations of microstructure and memory but not volumetric changes suggests that MRI derived microstructure measurements are superior to volume for detecting subtle changes. While this study did not include biomarkers of pathology such as amyloid or tau PET imaging, the microstructural-memory association was not found for the APOE ε4 noncarriers suggesting our results more likely represent a propensity of group-level early pathological changes that is occurring in individuals in the at-risk group.

Left subiculum microstructure was most strongly correlated with verbal memory performance. Greater subicular functional MRI activation during memory retrieval (Gabrieli et al., 1997; Ledergerber et al., 2021) and volumetric studies implicate subicular atrophy with delayed memory performance in older adults (Chi et al., 2022; Zammit et al., 2017) and individuals at-risk for developing AD (Carlesimo et al., 2015) support the roles of the subiculum in memory decline. Volumetric studies found reduced left subiculum volumes associated with poorer performance in delayed verbal recall in APOE ε4 carriers who had converted to mild cognitive impairment (Abraham et al., 2020) and in individuals with subjective cognitive decline (Zhao et al., 2019) and AD (Sarica et al., 2018). While in early studies CA1 atrophy was the best predictor of AD progression, we did not find any significant CA1 associations.

In its simplest form, diffusion weighted imaging can be made sensitive to the *apparent* diffusivity of water within tissue quantified as the apparent diffusion coefficient (ADC) which reflects the true self-diffusion coefficient of water weighted by the boundary-driven restriction of water displacement within a voxel. In complex biologic tissue like brain where microstructural boundaries like myelin sheaths can preferentially restrict water displacement in one direction (radial) and permit displacement in another (axial), diffusion can be restricted as a function of direction. When collected at various angles relative to the tissue, apparent diffusivity can vary as a function of tissue microstructure and angle of diffusion weighting. This phenomenon typically is quantified by the collection of multiple diffusion-weighted volumes, each with a diffusion weighting vector pointed in a different direction in space, and the calculation of a tensor to determine the mean diffusivity, degree of anisotropy, and principal direction of diffusion within individual voxels. This method is ubiquitous in academic and clinical research of AD pathogenesis (Chen et al., 2023; Cheng et al., 2023; Lancaster et al., 2016; Maggipinto et al., 2017; Zhu et al., 2015) . However, DTI sensitivity to early AD-associated microstructural deficits specificity to precise cell structure differences are lacking due to the nature of DTI, which is a quantitative representation of the *diffusion signal*. NODDI models of multi-shell diffusion data overcomes this limitation because it is a biophysical model design to quantify tangible microstructure (e.g., neurite density and orientation).

Hippocampal microstructure rather than volume was more sensitive to memory performance in APOE ε4 carriers, but the specific biological mechanisms underlying these associations remain unclear. Given that all of the participants are still considered unimpaired behaviorally, the findings reflected a relationship with memory functioning rather than group differences and the findings were for the ODI but not NDI metric. It is possible that since the subiculum is a main efferent pathway, memory performance is more tightly linked to the measurement of less dispersed neurons and better connectivity. NDI is commonly interpreted as a marker of neurite density and tissue integrity, so this suggests that other microstructural properties—such as myelination—may play a more prominent role in detecting early memory decline. Prior research (Fukutomi et al., 2019) has shown that NDI is inversely related to MD, a measure often linked to overall microstructural degradation (Vernooij et al., 2009). This aligns with evidence that hippocampal connectivity and fiber structure,

rather than solely neuronal packing density, are critical for memory function (Nazeri et al., 2015). Both ODI and FA were associated with memory performance, but ODI demonstrated a slightly stronger correlation, suggesting that NODDI may provide greater sensitivity to subtle hippocampal microstructural changes than traditional DTI metrics. Our findings suggest that while traditional DTI metrics capture basic diffusion properties, incorporating advanced models like NODDI may provide deeper insights into microstructural contributions to cognition.

Rational design of dMRI experiments and biophysical modelling of restricted diffusion within tissues (and the expected dMRI signal in such a modelled system), allows for non-invasive quantification of specific microstructure. In this case, we employed the well-established NODDI model and previous efforts have shown that NODDI measures correlated with tau pathology and neurodegeneration in a mouse model (Colgan et al., 2016) and MCI and AD patients' white matter difference (Fu et al., 2020) while DTI measures did not. In other studies, ODI has been shown to positively correlated with a PET biomarker of postsynaptic density (Mak et al., 2021), thus it is plausible to speculate that the ODI measures in this study are suggestive of very early loss of synaptic density in cognitively intact APOE ε4 carriers.

The NODDI model has limitations that include its inability to account for the diffusion signal contribution from tissue constituent microstructures, which may render gray matter too complex for NODDI's simplified model to accurately quantify the diffusion signal from dendrites alone. Larger datasets that support more sophisticated models of diffusion in brain, such as the Neurite Exchange Imaging (Jelescu et al., 2022) and the Soma and Neurite Density Imaging (Palombo et al., 2020) models, which account for exchange of water between compartments and the diffusion signal contribution from the soma, respectively will help address this limitation.

Acknowledgements

The authors thank Dr. Brian Gordon for generously providing his older adult brain atlas and guidance on coregistration methodology during image preprocessing.

References

Abraham, M., Seidenberg, M., Kelly, D.A., Nielson, K.A., Woodard, J.L., Carson Smith, J., Durgerian, S., Rao, S.M., 2020. Episodic Memory and Hippocampal Volume Predict 5-Year Mild Cognitive Impairment Conversion in Healthy Apolipoprotein ε4 Carriers. Journal of the International Neuropsychological Society 26, 733–738. https://doi.org/DOI: 10.1017/S1355617720000181

Adler, D.H., Pluta, J., Kadivar, S., Craige, C., Gee, J.C., Avants, B.B., Yushkevich, P.A., 2014. Histology-derived volumetric annotation of the human hippocampal subfields in postmortem MRI. Neuroimage 84, 505–523. https://doi.org/10.1016/j.neuroimage.2013.08.067

Apostolova, L.G., Dutton, R.A., Dinov, I.D., Hayashi, K.M., Toga, A.W., Cummings, J.L., Thompson, P.M., 2006. Conversion of Mild Cognitive Impairment to Alzheimer Disease Predicted by Hippocampal Atrophy Maps. Arch Neurol 63, 693. https://doi.org/10.1001/archneur.63.5.693

Baxter, L.C., Limback-Stokin, M., Patten, K.J., Arreola, A.C., Locke, D.E.C., Hu, L., Zhou, Y., Caselli, R.J., 2023. Hippocampal connectivity and memory decline in cognitively intact APOE ε4 carriers. Alzheimer's & Dementia n/a. https://doi.org/https://doi.org/10.1002/alz.13023

Carlesimo, G.A., Piras, F., Orfei, M.D., Iorio, M., Caltagirone, C., Spalletta, G., 2015. Atrophy of presubiculum and subiculum is the earliest hippocampal anatomical marker of Alzheimer's disease. Alzheimer's & Dementia: Diagnosis, Assessment & Disease Monitoring 1, 24–32. https://doi.org/10.1016/j.dadm.2014.12.001

Caselli, R.J., Dueck, A.C., Locke, D.E.C., Hoffman-Snyder, C.R., Woodruff, B.K., Rapcsak, S.Z., Reiman, E.M., 2011. Longitudinal modeling of frontal cognition in APOE 4 homozygotes, heterozygotes, and noncarriers. Neurology 76, 1383–1388. https://doi.org/10.1212/WNL.0b013e3182167147

Caselli, R.J., Dueck, A.C., Osborne, D., Sabbagh, M.N., Connor, D.J., Ahern, G.L., Baxter, L.C., Rapcsak, S.Z., Shi, J., Woodruff, B.K., Locke, D.E.C., Snyder, C.H., Alexander, G.E., Rademakers, R., Reiman, E.M., 2009. Longitudinal Modeling of Age-Related Memory Decline and the APOE ε4 Effect. New England Journal of Medicine 361, 255–263. https://doi.org/10.1056/NEJMoa0809437

Caselli, R.J., Walker, D., Sue, L., Sabbagh, M., Beach, T., 2010. Amyloid load in nondemented brains correlates with APOE ε4. Neurosci Lett 473, 168–171. https://doi.org/10.1016/j.neulet.2010.02.016

Chang, W.-T., Langella, S.K., Tang, Y., Ahmad, S., Zhang, H., Yap, P.-T., Giovanello, K.S., Lin, W., 2021. Brainwide functional networks associated with anatomically- and functionally-defined hippocampal subfields using ultrahigh-resolution fMRI. Sci Rep 11, 10835. https://doi.org/10.1038/s41598-021-90364-7

Chen, Y., Wang, Y., Song, Z., Fan, Y., Gao, T., Tang, X., 2023. Abnormal white matter changes in Alzheimer's disease based on diffusion tensor imaging: A systematic review. Ageing Res Rev 87, 101911. https://doi.org/https://doi.org/10.1016/j.arr.2023.101911

Cheng, X., Li, D., Peng, J., Shu, Z., Xing, X., 2023. Prediction of MCI progression to AD based on DTI-derived diffusion parameters: construction and validation of a nomogram. Eur Neurol 1. https://doi.org/10.1159/000534767

Chi, C.-H., Yang, F.-C., Chang, Y.-L., 2022. Age-related volumetric alterations in hippocampal subiculum region are associated with reduced retention of the "when" memory component. Brain Cogn 160, 105877. https://doi.org/https://doi.org/10.1016/j.bandc.2022.105877

Colgan, N., Siow, B., O'Callaghan, J.M., Harrison, I.F., Wells, J.A., Holmes, H.E., Ismail, O., Richardson, S., Alexander, D.C., Collins, E.C., Fisher, E.M., Johnson, R., Schwarz, A.J., Ahmed, Z., O'Neill, M.J., Murray, T.K., Zhang, H., Lythgoe, M.F., 2016. Application of neurite orientation dispersion and density imaging (NODDI) to a tau pathology model of Alzheimer's disease. Neuroimage 125, 739–744. https://doi.org/10.1016/j.neuroimage.2015.10.043

de Flores, R., la Joie, R., Chételat, G., 2015. Structural imaging of hippocampal subfields in healthy aging and Alzheimer's disease. Neuroscience 309, 29–50. https://doi.org/https://doi.org/10.1016/j.neuroscience.2015.08.033

Desikan, R.S., Ségonne, F., Fischl, B., Quinn, B.T., Dickerson, B.C., Blacker, D., Buckner, R.L., Dale, A.M., Maguire, R.P., Hyman, B.T., Albert, M.S., Killiany, R.J., 2006. An automated labeling system for

subdividing the human cerebral cortex on MRI scans into gyral based regions of interest. Neuroimage 31, 968–980. https://doi.org/10.1016/j.neuroimage.2006.01.021

Flores, R., Berron, D., Ding, S., Ittyerah, R., Pluta, J.B., Xie, L., Adler, D.H., Robinson, J.L., Schuck, T., Trojanowski, J.Q., Grossman, M., Liu, W., Pickup, S., Das, S.R., Wolk, D.A., Yushkevich, P.A., Wisse, L.E.M., 2020. Characterization of hippocampal subfields using ex vivo MRI and histology data: Lessons for in vivo segmentation. Hippocampus 30, 545–564. https://doi.org/10.1002/hipo.23172

Folstein, M.F., Folstein, S.E., McHugh, P.R., 1975. "Mini-Mental State". A practical method for grading the cognitive state of patients for the clinician. J Psychiatr Res 12, 189–198. https://doi.org/10.1016/0022-3956(75)90026-6

Frazier, J.A., Chiu, S., Breeze, J.L., Makris, N., Lange, N., Kennedy, D.N., Herbert, M.R., Bent, E.K., Koneru, V.K., Dieterich, M.E., Hodge, S.M., Rauch, S.L., Grant, P.E., Cohen, B.M., Seidman, L.J., Caviness, V.S., Biederman, J., 2005. Structural Brain Magnetic Resonance Imaging of Limbic and Thalamic Volumes in Pediatric Bipolar Disorder. American Journal of Psychiatry 162, 1256–1265. https://doi.org/10.1176/appi.ajp.162.7.1256

Fu, X., Shrestha, S., Sun, M., Wu, Q., Luo, Y., Zhang, X., Yin, J., Ni, H., 2020. Microstructural White Matter Alterations in Mild Cognitive Impairment and Alzheimer's Disease. Clin Neuroradiol 30, 569–579. https://doi.org/10.1007/s00062-019-00805-0

Gabrieli, J.D.E., Brewer, J.B., Desmond, J.E., Glover, G.H., 1997. Separate Neural Bases of Two Fundamental Memory Processes in the Human Medial Temporal Lobe. Science (1979) 276, 264–266.

Gordon, B.A., Blazey, T., Benzinger, T.L.S., Head, D., 2013. Effects of Aging and Alzheimer's Disease Along the Longitudinal Axis of the Hippocampus. Journal of Alzheimer's Disease 37, 41–50. https://doi.org/10.3233/JAD-130011

Gordon, B.A., Zacks, J.M., Blazey, T., Benzinger, T.L.S., Morris, J.C., Fagan, A.M., Holtzman, D.M., Balota, D.A., 2015. Task-evoked fMRI changes in attention networks are associated with preclinical Alzheimer's disease biomarkers. Neurobiol Aging 36, 1771–1779. https://doi.org/https://doi.org/10.1016/j.neurobiolaging.2015.01.019

Hamilton, M., 1967. Development of a Rating Scale for Primary Depressive Illness. British Journal of Social and Clinical Psychology 6, 278–296. https://doi.org/10.1111/j.2044-8260.1967.tb00530.x

Hesse, R., Hurtado, M.L., Jackson, R.J., Eaton, S.L., Herrmann, A.G., Colom-Cadena, M., Tzioras, M., King, D., Rose, J., Tulloch, J., McKenzie, C.-A., Smith, C., Henstridge, C.M., Lamont, D., Wishart, T.M., Spires-Jones, T.L., 2019. Comparative profiling of the synaptic proteome from Alzheimer's disease patients with focus on the APOE genotype. Acta Neuropathol Commun 7, 214. https://doi.org/10.1186/s40478-019-0847-7

Hett, K., Ta, V.-T., Catheline, G., Tourdias, T., Manjón, J. v., Coupé, P., Weiner, M.W., Aisen, P., Petersen, R., Jack, C.R., Jagust, W., Trojanowki, J.Q., Toga, A.W., Beckett, L., Green, R.C., Saykin, A.J., Morris, J., Shaw, L.M., Khachaturian, Z., Sorensen, G., Carrillo, M., Kuller, L., Raichle, M., Paul, S., Davies, P., Fillit, H., Hefti, F., Holtzman, D., Mesulam, M.M., Potter, W., Snyder, P., Montine, T., Thomas, R.G., Donohue, M., Walter, S., Sather, T., Jiminez, G., Balasubramanian, A.B., Mason, J., Sim, I., Harvey, D., Bernstein, M., Fox, N., Thompson, P., Schuff, N., DeCArli, C., Borowski, B., Gunter, J., Senjem, M., Vemuri, P., Jones, D., Kantarci, K., Ward, C., Koeppe, R.A., Foster, N., Reiman, E.M., Chen, K., Mathis, C., Landau, S., Cairns, N.J., Householder, E., Taylor-Reinwald, L., Lee, V., Korecka, M., Figurski, M., Crawford, K., Neu, S., Foroud, T.M., Potkin, S., Shen, L., Faber, K., Kim, S., Nho, K., Thal, L., Frank, R., Hsiao, J., Kaye, J., Quinn, J., Silbert, L., Lind, B., Carter, R., Dolen, S., Ances, B., Carroll, M., Creech, M.L., Franklin, E., Mintun, M.A., Schneider, S., Oliver, A., Schneider, L.S., Pawluczyk, S., Beccera, M., Teodoro, L., Spann, B.M., Brewer, J., Vanderswag, H., Fleisher, A., Marson, D., Griffith, R., Clark, D., Geldmacher, D., Brockington, J., Roberson, E., Love, M.N., Heidebrink, J.L., Lord, J.L., Mason, S.S., Albers, C.S., Knopman, D., Johnson, Kris, Grossman, H., Mitsis, E., Shah, R.C., deToledo-Morrell, L., Doody, R.S., Villanueva-Meyer, J., Chowdhury, M., Rountree, S., Dang, M., Duara, R., Varon, D., Greig, M.T., Roberts, P., Stern, Y., Honig, L.S., Bell, K.L., Albert, M., Onyike, C., D'Agostino, D., Kielb, S., Galvin, J.E., Cerbone, B., Michel, C.A., Pogorelec, D.M., Rusinek, H., de Leon, M.J., Glodzik, L., de Santi, S., Womack, K., Mathews, D., Quiceno, M., Doraiswamy, P.M., Petrella, J.R., Borges-Neto, S., Wong, T.Z., Coleman, E., Levey, A.I., Lah, J.J., Cella, J.S., Burns, J.M., Swerdlow, R.H., Brooks, W.M.,

Arnold, S.E., Karlawish, J.H., Wolk, D., Clark, C.M., Apostolova, L., Tingus, K., Woo, E., Silverman, D.H.S., Lu, P.H., Bartzokis, G., Smith, C.D., Jicha, G., Hardy, P., Sinha, P., Oates, E., Conrad, G., Graff-Radford, N.R., Parfitt, F., Kendall, T., Johnson, H., Lopez, O.L., Oakley, M., Simpson, D.M., Farlow, M.R., Hake, A.M., Matthews, B.R., Brosch, J.R., Herring, S., Hunt, C., Porsteinsson, A.P., Goldstein, B.S., Martin, K., Makino, K.M., Ismail, M.S., Brand, C., Mulnard, R.A., Thai, G., Mc-Adams-Ortiz, C., van Dyck, C.H., Carson, R.E., MacAvoy, M.G., Varma, P., Chertkow, H., Bergman, H., Hosein, C., Black, S., Stefanovic, B., Caldwell, C., Hsiung, G.-Y.R., Feldman, H., Mudge, B., Assaly, M., Finger, Elizabeth, Pasternack, S., Rachisky, I., Trost, D., Kertesz, A., Bernick, C., Munic, D., Lipowski, K., Weintraub, M.A.S., Bonakdarpour, B., Kerwin, D., Wu, C.-K., Johnson, N., Sadowsky, C., Villena, T., Turner, R.S., Johnson, Kathleen, Reynolds, B., Sperling, R.A., Johnson, K.A., Marshall, G., Yesavage, J., Taylor, J.L., Lane, B., Rosen, A., Tinklenberg, J., Sabbagh, M.N., Belden, C.M., Jacobson, S.A., Sirrel, S.A., Kowall, N., Killiany, R., Budson, A.E., Norbash, A., Johnson, P.L., Obisesan, T.O., Wolday, S., Allard, J., Lerner, A., Ogrocki, P., Tatsuoka, C., Fatica, P., Fletcher, E., Maillard, P., Olichney, J., Carmichael, O., Kittur, S., Borrie, M., Lee, T.-Y., Bartha, R., Johnson, S., Asthana, S., Carlsson, C.M., Preda, A., Nguyen, D., Tariot, P., Burke, A., Trncic, N., Fleisher, A., Reeder, S., Bates, V., Capote, H., Rainka, M., Scharre, D.W., Kataki, M., Adeli, A., Zimmerman, E.A., Celmins, D., Brown, A.D., Pearlson, G.D., Blank, K., Anderson, K., Flashman, L.A., Seltzer, M., Hynes, M.L., Santulli, R.B., Sink, K.M., Gordineer, L., Williamson, J.D., Garg, P., Watkins, F., Ott, B.R., Querfurth, H., Tremont, G., Salloway, S., Malloy, P., Correia, S., Rosen, H.J., Miller, B.L., Perry, D., Mintzer, J., Spicer, K., Bachman, D., Finger, Elizabether, Pasternak, S., Rachinsky, I., Rogers, J., Drost, D., Pomara, N., Hernando, R., Sarrael, A., Schultz, S.K., Boles Ponto, L.L., Shim, H., Smith, K.E., Relkin, N., Chaing, G., Lin, M., Ravdin, L., Smith, A., Raj, B.A., Fargher, K., 2019. Multimodal Hippocampal Subfield Grading For Alzheimer's Disease Classification. Sci Rep 9, 13845. https://doi.org/10.1038/s41598-019-49970-9

Iglesias, J.E., Augustinack, J.C., Nguyen, K., Player, C.M., Player, A., Wright, M., Roy, N., Frosch, M.P., McKee, A.C., Wald, L.L., Fischl, B., Van Leemput, K., 2015. A computational atlas of the hippocampal formation using ex vivo, ultra-high resolution MRI: Application to adaptive segmentation of in vivo MRI. Neuroimage 115, 117–137. https://doi.org/https://doi.org/10.1016/j.neuroimage.2015.04.042

Jelescu, I.O., de Skowronski, A., Geffroy, F., Palombo, M., Novikov, D.S., 2022. Neurite Exchange Imaging (NEXI): A minimal model of diffusion in gray matter with inter-compartment water exchange. Neuroimage 256, 119277. https://doi.org/https://doi.org/10.1016/j.neuroimage.2022.119277

Jessen, F., Feyen, L., Freymann, K., Tepest, R., Maier, W., Heun, R., Schild, H.-H., Scheef, L., 2006. Volume reduction of the entorhinal cortex in subjective memory impairment. Neurobiol Aging 27, 1751–1756. https://doi.org/10.1016/j.neurobiolaging.2005.10.010

Kashyap, G., Bapat, D., Das, D., Gowaikar, R., Amritkar, R.E., Rangarajan, G., Ravindranath, V., Ambika, G., 2019. Synapse loss and progress of Alzheimer's disease -A network model. Sci Rep 9, 6555. https://doi.org/10.1038/s41598-019-43076-y

Katz, S., Downs, T.D., Cash, H.R., Grotz, R.C., 1970. Progress in development of the Index of ADL1. Gerontologist 10, 20–30.

Koffie, R.M., Hashimoto, T., Tai, H.-C., Kay, K.R., Serrano-Pozo, A., Joyner, D., Hou, S., Kopeikina, K.J., Frosch, M.P., Lee, V.M., Holtzman, D.M., Hyman, B.T., Spires-Jones, T.L., 2012. Apolipoprotein E4 effects in Alzheimer's disease are mediated by synaptotoxic oligomeric amyloid-β. Brain 135, 2155–2168. https://doi.org/10.1093/brain/aws127

Kohli, A., DiFilippo, A.H., Gallagher, R.L., Davenport, N.J., Betthauser, T.J., Johnson, S.C., Christian, B.T., Bendlin, B.B., 2021. Neurite density and free water concentration are associated with synaptic density in the hippocampus as assessed through NODDI and [C-11]UCB-J PET. Alzheimer's & Dementia 17, e054042. https://doi.org/https://doi.org/10.1002/alz.054042

Lancaster, M.A., Seidenberg, M., Smith, J.C., Nielson, K.A., Woodard, J.L., Durgerian, S., Rao, S.M., 2016. Diffusion Tensor Imaging Predictors of Episodic Memory Decline in Healthy Elders at Genetic Risk for Alzheimer's Disease. Journal of the International Neuropsychological Society 22, 1005–1015. https://doi.org/10.1017/S1355617716000904

Lane-Donovan, C., Herz, J., 2017. ApoE, ApoE Receptors, and the Synapse in Alzheimer's Disease. Trends Endocrinol Metab 28, 273–284. https://doi.org/10.1016/j.tem.2016.12.001

Ledergerber, D., Battistin, C., Blackstad, J.S., Gardner, R.J., Witter, M.P., Moser, M.-B., Roudi, Y., Moser, E.I., 2021. Task-dependent mixed selectivity in the subiculum. Cell Rep 35, 109175. https://doi.org/10.1016/j.celrep.2021.109175

Li, S., Selkoe, D.J., 2020. A mechanistic hypothesis for the impairment of synaptic plasticity by soluble Aβ oligomers from Alzheimer's brain. J Neurochem 154, 583–597. https://doi.org/10.1111/jnc.15007

Lindberg, O., Mårtensson, G., Stomrud, E., Palmqvist, S., Wahlund, L.-O., Westman, E., Hansson, O., 2017. Atrophy of the Posterior Subiculum Is Associated with Memory Impairment, Tau- and Aβ Pathology in Non-demented Individuals. Front Aging Neurosci 9. https://doi.org/10.3389/fnagi.2017.00306

Maggipinto, T., Bellotti, R., Amoroso, N., Diacono, D., Donvito, G., Lella, E., Monaco, A., Antonella Scelsi, M., Tangaro, S., Initiative, for the A.D.N., 2017. DTI measurements for Alzheimer's classification. Phys Med Biol 62, 2361. https://doi.org/10.1088/1361-6560/aa5dbe

Mak, E., Holland, N., Jones, P.S., Savulich, G., Low, A., Malpetti, M., Kaalund, S.S., Passamonti, L., Rittman, T., Romero-Garcia, R., Manavaki, R., Williams, G.B., Hong, Y.T., Fryer, T.D., Aigbirhio, F.I., O'Brien, J.T., Rowe, J.B., 2021. In vivo coupling of dendritic complexity with presynaptic density in primary tauopathies. Neurobiol Aging 101, 187–198. https://doi.org/10.1016/j.neurobiolaging.2021.01.016

Makris, N., Goldstein, J.M., Kennedy, D., Hodge, S.M., Caviness, V.S., Faraone, S. v., Tsuang, M.T., Seidman, L.J., 2006. Decreased volume of left and total anterior insular lobule in schizophrenia. Schizophr Res 83, 155–171. https://doi.org/10.1016/j.schres.2005.11.020

Mohtasib, R., Alghamdi, J., Jobeir, A., Masawi, A., Pedrosa de Barros, N., Billiet, T., Struyfs, H., Phan, T. v, van Hecke, W., Ribbens, A., 2022. MRI biomarkers for Alzheimer's disease: the impact of functional connectivity in the default mode network and structural connectivity between lobes on diagnostic accuracy. Heliyon 8, e08901. https://doi.org/https://doi.org/10.1016/j.heliyon.2022.e08901

Nelson, L., Tabet, N., 2015. Slowing the progression of Alzheimer's disease; what works? Ageing Res Rev 23, 193–209. https://doi.org/10.1016/j.arr.2015.07.002

Palombo, M., Ianus, A., Guerreri, M., Nunes, D., Alexander, D.C., Shemesh, N., Zhang, H., 2020. SANDI: A compartment-based model for non-invasive apparent soma and neurite imaging by diffusion MRI. Neuroimage 215, 116835. https://doi.org/10.1016/j.neuroimage.2020.116835

Parker, C.S., Veale, T., Bocchetta, M., Slattery, C.F., Malone, I.B., Thomas, D.L., Schott, J.M., Cash, D.M., Zhang, H., 2021. Not all voxels are created equal: Reducing estimation bias in regional NODDI metrics using tissue-weighted means. Neuroimage 245, 118749. https://doi.org/10.1016/j.neuroimage.2021.118749

Reiman, E.M., Uecker, A., Caselli, R.J., Lewis, S., Bandy, D., de Leon, M.J., de Santi, S., Convit, A., Osborne, D., Weaver, A., Thibodeau, S.N., 1998. Hippocampal volumes in cognitively normal persons at genetic risk for Alzheimer's disease. Ann Neurol 44, 288–291. https://doi.org/10.1002/ana.410440226

Sarica, A., Vasta, R., Novellino, F., Vaccaro, M.G., Cerasa, A., Quattrone, A., 2018. MRI Asymmetry Index of Hippocampal Subfields Increases Through the Continuum From the Mild Cognitive Impairment to the Alzheimer's Disease. Front Neurosci 12. https://doi.org/10.3389/fnins.2018.00576

Schilling, K.G., Blaber, J., Hansen, C., Cai, L., Rogers, B., Anderson, A.W., Smith, S., Kanakaraj, P., Rex, T., Resnick, S.M., Shafer, A.T., Cutting, L.E., Woodward, N., Zald, D., Landman, B.A., 2020. Distortion correction of diffusion weighted MRI without reverse phase-encoding scans or field-maps. PLoS One 15, e0236418. https://doi.org/10.1371/journal.pone.0236418

Sheng, M., Sabatini, B.L., Sudhof, T.C., 2012. Synapses and Alzheimer's Disease. Cold Spring Harb Perspect Biol 4, a005777–a005777. https://doi.org/10.1101/cshperspect.a005777

Tournier, J.-D., Smith, R., Raffelt, D., Tabbara, R., Dhollander, T., Pietsch, M., Christiaens, D., Jeurissen, B., Yeh, C.-H., Connelly, A., 2019. MRtrix3: A fast, flexible and open software framework for medical image processing and visualisation. Neuroimage 202, 116137. https://doi.org/10.1016/j.neuroimage.2019.116137

Vogt, N.M., Hunt, J.F., Adluru, N., Dean, D.C., Johnson, S.C., Asthana, S., Yu, J.-P.J., Alexander, A.L., Bendlin, B.B., 2020. Cortical Microstructural Alterations in Mild Cognitive Impairment and Alzheimer's Disease Dementia. Cerebral Cortex 30, 2948–2960. https://doi.org/10.1093/cercor/bhz286

Zammit, A.R., Ezzati, A., Zimmerman, M.E., Lipton, R.B., Lipton, M.L., Katz, M.J., 2017. Roles of hippocampal subfields in verbal and visual episodic memory. Behavioural Brain Research 317, 157–162. https://doi.org/10.1016/j.bbr.2016.09.038

Zhang, H., Schneider, T., Wheeler-Kingshott, C.A., Alexander, D.C., 2012. NODDI: Practical in vivo neurite orientation dispersion and density imaging of the human brain. Neuroimage 61, 1000–1016. https://doi.org/10.1016/j.neuroimage.2012.03.072

Zhao, W., Wang, X., Yin, C., He, M., Li, S., Han, Y., 2019. Trajectories of the Hippocampal Subfields Atrophy in the Alzheimer's Disease: A Structural Imaging Study. Front Neuroinform 13. https://doi.org/10.3389/fninf.2019.00013

Zhu, Q.-Y., Bi, S.-W., Yao, X.-T., Ni, Z.-Y., Li, Y., Chen, B.-Y., Fan, G.-G., Shang, X.-L., 2015. Disruption of thalamic connectivity in Alzheimer's disease: a diffusion tensor imaging study. Metab Brain Dis 30, 1295–1308. https://doi.org/10.1007/s11011-015-9708-7

Fukutomi, H., Glasser, M. F., Murata, K., Akasaka, T., Fujimoto, K., Yamamoto, T., Autio, J. A., Okada, T., Togashi, K., Zhang, H., Van Essen, D. C., & Hayashi, T. (2019). Diffusion Tensor Model links to Neurite Orientation Dispersion and Density Imaging at high b-value in Cerebral Cortical Gray Matter. Scientific Reports, 9(1), 12246. https://doi.org/10.1038/s41598-019-48671-7

Jelescu, I. O., Palombo, M., Bagnato, F., & Schilling, K. G. (2020). Challenges for biophysical modeling of microstructure. Journal of Neuroscience Methods, 344, 108861. https://doi.org/10.1016/j.jneumeth.2020.108861

Nazeri, A., Chakravarty, M. M., Rotenberg, D. J., Rajji, T. K., Rathi, Y., Michailovich, O. V., & Voineskos, A. N. (2015). Functional Consequences of Neurite Orientation Dispersion and Density in Humans across the Adult Lifespan. Journal of Neuroscience, 35(4), 1753–1762. https://doi.org/10.1523/JNEUROSCI.3979-14.2015

Parker, C. S., Veale, T., Bocchetta, M., Slattery, C. F., Malone, I. B., Thomas, D. L., Schott, J. M., Cash, D. M., & Zhang, H. (2021). Not all voxels are created equal: Reducing estimation bias in regional NODDI metrics using tissue-weighted means. NeuroImage, 245, 118749. https://doi.org/10.1016/J.NEUROIMAGE.2021.118749

Qiu, A., Alexander, A. L., Edwards, L. J., Pine, K. J., Ellerbrock, I., Weiskopf, N., & Mohammadi, S. (2017). NODDI-DTI: Estimating Neurite Orientation and Dispersion Parameters from a Diffusion Tensor in Healthy White Matter. Frontiers in Neuroscience | Www.Frontiersin.Org, 11. https://doi.org/10.3389/fnins.2017.00720

Thompson, P. M., Hayashi, K. M., de Zubicaray, G., Janke, A. L., Rose, S. E., Semple, J., Herman, D., Hong, M. S., Dittmer, S. S., Doddrell, D. M., & Toga, A. W. (2003). Dynamics of gray matter loss in Alzheimer's disease. The Journal of Neuroscience: The Official Journal of the Society for Neuroscience, 23(3), 994–1005. https://doi.org/10.1523/JNEUROSCI.23-03-00994.2003

Vernooij, M. W., Ikram, M. A., Vrooman, H. A., Wielopolski, P. A., Krestin, G. P., Hofman, A., Niessen, W. J., Van der Lugt, A., & Breteler, M. M. B. (2009). White Matter Microstructural Integrity and Cognitive Function in a General Elderly Population. Archives of General Psychiatry, 66(5), 545–553. https://doi.org/10.1001/archgenpsychiatry.2009.5

Table 1. Demographic and NODDI data.

	Carriers	Noncarriers
	(n = 33)	(n = 41)
APOE ε4 genotype	4-2 = 1; 4-3 = 29; 4-4 = 9	3-2 = 3; 3-3 = 50
Age years mean/SD (range)	71.2/ (60-88)	71.4/6.5 (60-84)
Gender (M/F) [%F]	2/31 [94% F]	10/31 [76%F]*
Education (years)	15.9 (2.0)	15.9 (2.2)
Handedness (R/L/A)	34/3/2	47/5/1
AVLT-DR (mean (SD))	7.94 (4.4)	9.02 (4.0)
RCF-DR score (mean (SD))	18.2 (7.3)	19.8 (7.0)
ODI hippocampal measures		
Left CA1	.40 (.09)	.39 (.08)
Left CA23	.24 (.05)	.24 (.06)
Left CA4/DG	.30 (.06)	.32 (.09)
Left subiculum	.43 (.06)	.45 (.06)
Left hippocampus	.36 (.06)	.37 (.05)
Right CA1	.43 (.08)	.42 (.09)
Right CA23	.23 (.07)	.25 (.09)
Right CA4/DG	.35 (.08)	.35 (.09)
Right subiculum	.39 (.05)	.36 (.05)
Right hippocampus	.36 (.05)	.37 (06)
NDI hippocampal measures		
Left CA1	.44 (.03)	.46 (.03)
Left CA23	.50 (.04)	.05 (.05)
Left CA4/DG	.17 (.04)	.47 (.05)
Left subiculum	.46 (.04)	.47 (.05)
Left hippocampus	.46 (.03)	.47 (.03)
Right CA1	.44 (.03)	.44 (.03)
Right CA23	.25 (.07)	.51 (.06)
Right CA4/DG	.46 (.05)	.46 (.04)
Right subiculum	.50 (.04)	.48 (.04)
Right hippocampus	.47 (.03)	.47 (.03)

* Gender: X^2 (2, N = 74) =4.5, p = .03; No other significant group differences observed. CA1, CA23: subfields of the cornu ammonis; DG: dentate gyrus

Table 2. Summary based on statistical relationship (multiple comparisons corrected p-values) between imaging metrics (ODI, FA and Volume) and cognitive test (AVLT and CFT).

Region	ODI &AVLT	ODI & CFT	FA & AVLT	FA & CFT	Volume & AVLT	Volume & CFT
Left CA1	0.4422	0.4124	0.5031	0.5885	0.143	0.694
Left CA2-3	0.0751	0.3465	0.0732	0.7168	0.6891	0.8925
Left CA4	0.1434	0.2407	0.1489	0.8012	0.4682	0.3778
Left Subiculum	**0.0011***	0.1827	0.0052	0.9779	0.9842	0.8756
Left Hippocampus	0.0563	0.2581	0.0562	0.8223	0.2507	0.6768
Right CA1	0.889	0.7	0.9639	0.616	0.0454	0.6568
Right CA2-3	0.7224	0.4853	0.892	0.6946	0.5224	0.5065
Right CA4	0.8312	0.8837	0.8909	0.623	0.032	0.1299
Right Subiculum	0.3073	0.2042	0.5942	0.8696	0.5728	0.492
Right Hippocampus	0.9749	0.7052	0.7458	0.6685	0.1193	0.9285

*p-values<0.05 are considered statistically significant

Table 3. Summary of statistical relationships (multiple comparisons corrected p-values and R^2 values) between imaging metrics (ODI, FA, and Volume) and cognitive performance (AVLT) in APOE-E4 carrier and non-carrier groups.

METRIC	APOE-E4 CARRIER STTAUS	R^2	p-value
FA	Non-carrier	0.0158	0.3842
FA	Carrier	0.2243	0.0018
ODI	Non-carrier	0.0256	0.2673
ODI	Carrier	0.2937	0.0003
Vol	Non-carrier	0.0001	0.9501
Vol	Carrier	0.002	0.7837

Figures

Figure 1A

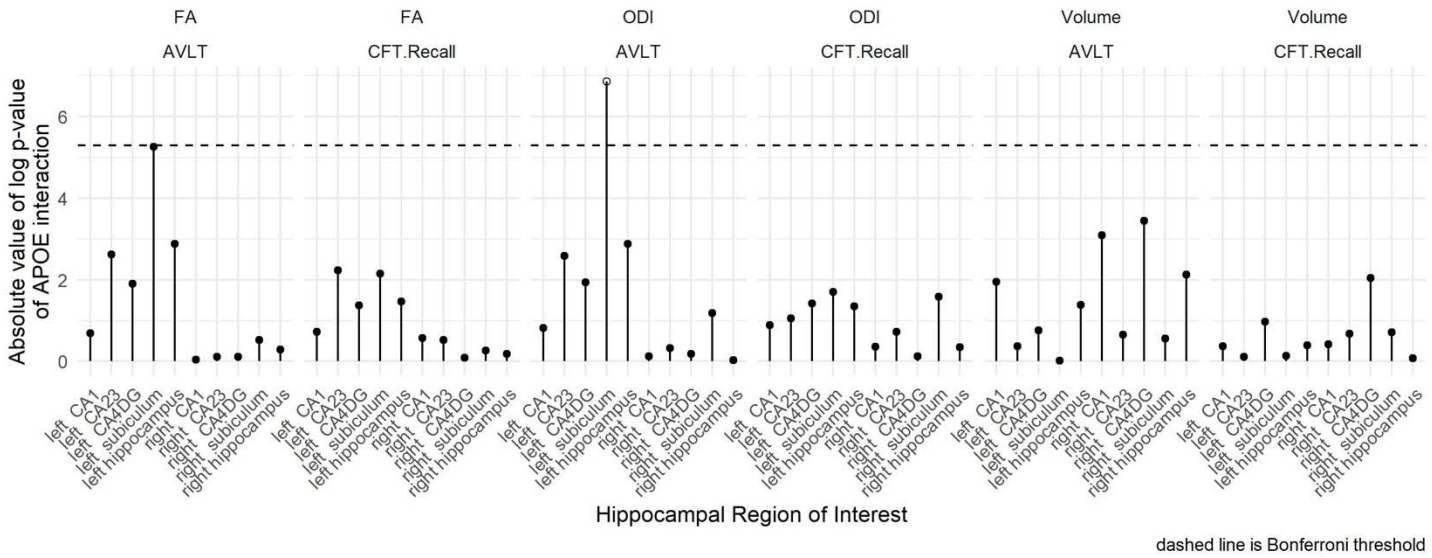

Figure 1B

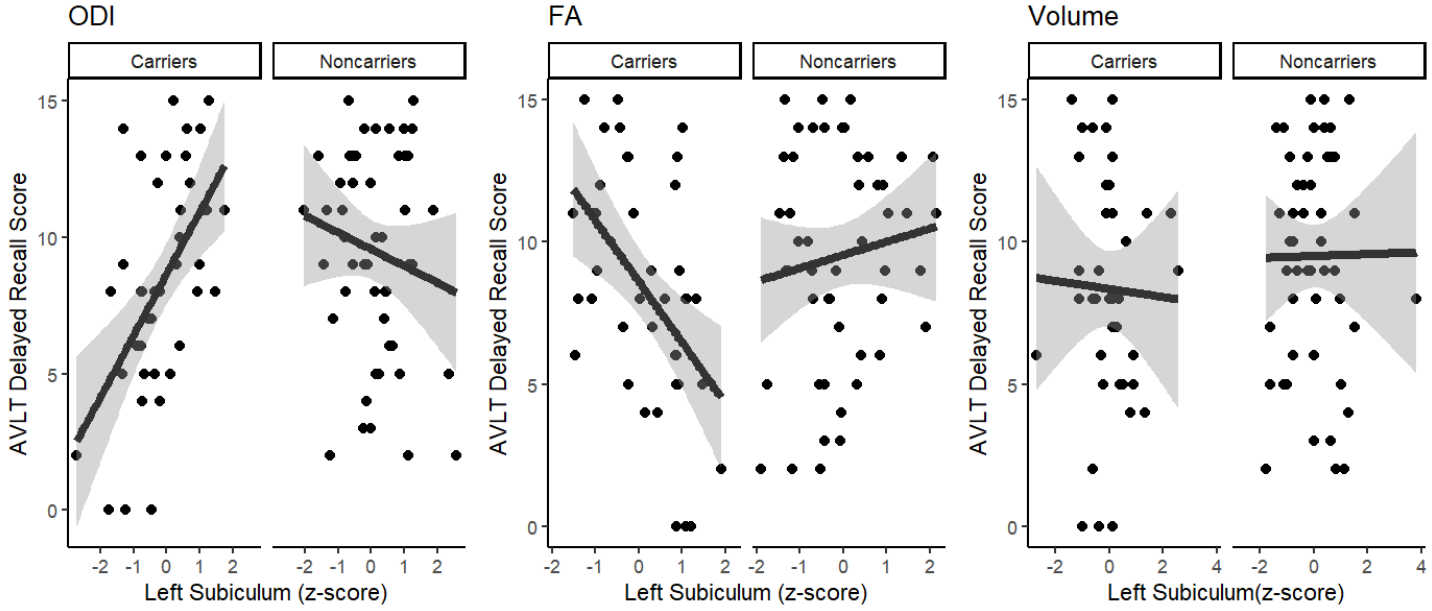

Figure captions

Figure 1A. Absolute values of log-transformed raw p-values for the APOE ε4 interaction across 10 hippocampal regions of interest (i.e., left and right CA1, CA2-3, CA4, subiculum and whole hippocampus), assessed for ODI, FA, and volume metrics in relation to AVLT and CFT delayed memory scores. Higher magnitudes correspond to smaller p-values. The dashed line represents the threshold for statistical significance after Bonferroni correction for 10 comparisons (p=0.005). Weaker left subiculum ODI was associated with lower AVLT scores.

Figure 1B. Correlations of left subiculum microstructure imaging metrics (NODDI-ODI and DTI-FA) and volume measures and memory scores by APOE ε4 groups showing that a correlation of lower left subiculum OID (z-score) with lower verbal memory scores was only found in APOE ε4 carriers.

Supplementary Data

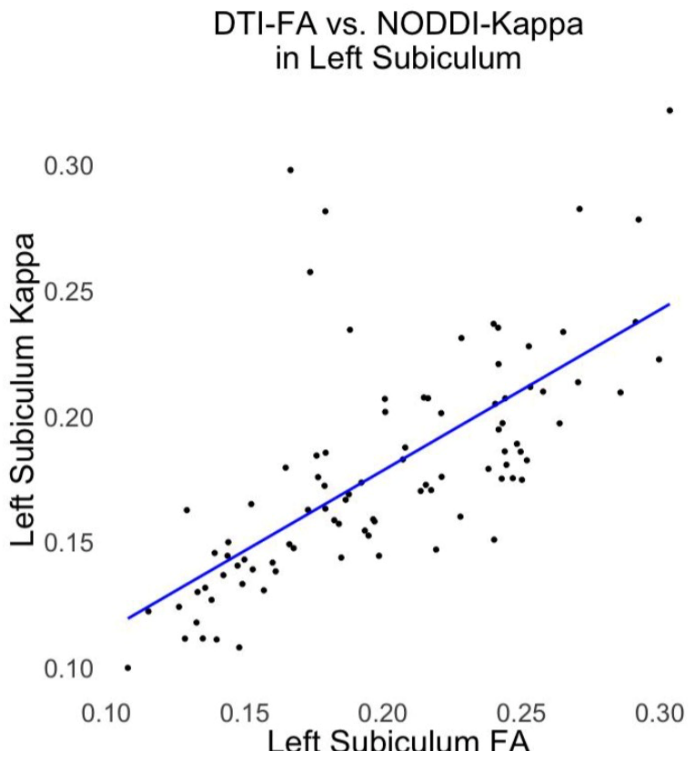

Figure S1. Scatter plot illustrating the relationship between DTI-FA and NODDI-Kappa in the left subiculum.